Numerical Study of the Packing of Wet Coarse Uniform Spheres

R. Y. Yang, R. P. Zou, and A. B. Yu
Centre for Computer Simulation and Modelling of Particulate Systems,
School of Materials Science and Engineering,
The University of New South Wales, Sydney, NSW 2052, Australia

The discrete-element method was extended to investigate the effect of liquid addition on the packing of monosized spheres. By explicitly taking into account the interaction forces between particles, such as contact forces and capillary force, the packing of wet spheres can be simulated by the method. Simulations are performed under the so-called poured packing, where a different amount of water is added to spheres of different sizes. Comparison with data in the literature shows that the simulations yield a satisfactory agreement in the relationship between porosity and moisture content, macroscopically verifying the proposed model. The packing structure is then analyzed in terms of microscopic properties such as the radial distribution function and coordination number and are shown to vary with liquid content for a given particle size. The relationship between porosity and capillary force is finally quantified, which confirms those derived based on macroscopic assumptions.

Introduction

Random packing of particles has been a subject of research for many years because of its fundamental importance in many engineering applications (German, 1989) and usefulness in modeling some physical systems (Bideau and Hansen, 1993; Metha, 1994). Previous studies have been concerned primarily with packings dominated by the gravity force. Under given packing conditions, this type of packing is controlled mainly by two factors: particle size distribution and shape. Therefore, many efforts have been made to develop an effective method for predicting the effects of the two factors on porosity and related packing properties, as reviewed by Yu and Zou (1998). However, in addition to the gravity force, other forces may also play an important role here. For example, it has been known that for particles of a size below 100 μm, the van der Waals force is more critical and affects the packing of particles remarkably at either the macroscopic or microscopic level (Yu et al., 1997; Yang et al., 2000).

Another force that usually gives a similar effect is the liquid-related force, for example, the capillary force. The packing behavior of wet particles is different from that of dry particles, as seen from the work on the packing of iron ore fines (Hinkley et al., 1994) or coal particles (Yu et al., 1995). In such packing, the capillary force is the intrinsic factor to influence the behavior of particles (Rumpf, 1962; Krupp, 1967; Visser, 1989). Therefore, understanding the effect of the capillary force is necessary for the optimum control of the packing of wet particles. Recent experimental studies of Feng and Yu (1998, 2000) have shown that there is an interrelationship between porosity, liquid content, and capillary force. Only the macroscopic packing properties can be obtained from their work, however, and the dependence of packing structure on the capillary force is still unknown. While steady progress has been made in the modeling of the packing of wet mono- or bi-sized spheres (Feng and Yu, 1998; Zou et al., 2001), much more fundamental work is required in order to develop a general predictive model for practical application.

Computer simulation has been widely used in the microscopic study of the packing of particles. Previous numerical techniques such as sequential addition or collective rearrangement involve various assumptions for packing growth and/or criteria for stability. These assumptions or criteria are largely derived from geometrical consideration and are applicable to the packing in which the gravity is the only effective force. They cannot be used in the simulation of the packing of particles, which depends on not only the gravity but also other forces, such as the van der Waals force associated with

Correspondence concerning this article should be addressed to A. B. Yu.

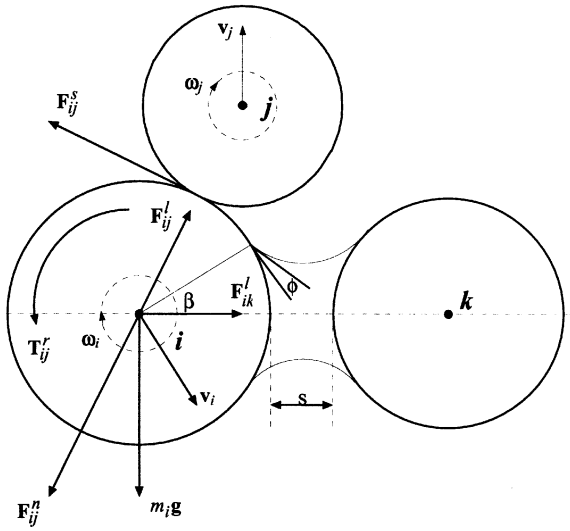

Figure 1. Forces acting on particle *i* from contacting particle *j* (for contact forces) and noncontacting particle *k* (for capillary force).

fine particles or capillary force associated with wet particles. Proper incorporation of these forces in a computer simulation is key to generating realistic packing. An effective way to achieve this goal is based on the discrete-element method (DEM) (Cundall and Stack, 1979), which treats particle packing as a dynamic process, and the interparticle forces are explicitly considered. The method, with some modifications, has been successfully used in the study of dry coarse or fine spheres (Liu et al., 1999; Yang et al., 2000; Zhang et al., 2001). In this article, the DEM approach will be extended to the packing of wet particles. The simulation conditions are similar to those used in the previous experimental work (Feng and Yu, 1998), so that the validity of the approach can be examined by comparing the simulated and measured results. The resulting packing structures are analyzed mainly in terms of the radial distribution function and coordination number.

Simulation Technique

Governing equation and force description

DEM simulation uses an explicit numerical scheme in which the motion of individual particles and their interaction with each other are traced (Cundall and Stack, 1979). The contact forces and capillary force are considered in the present simulation, as illustrated in Figure 1. Thus, the movement of particle i of radius R_i and mass m_i in a time step can be computed based on the integration of Newton's law of motion given by

$$m_i \frac{d\boldsymbol{v}_i}{dt} = \sum_j \left(\boldsymbol{F}_{ij}^n + \boldsymbol{F}_{ij}^s + \boldsymbol{F}_{ij}^l \right) + m_i \boldsymbol{g} \tag{1}$$

$$I_i \frac{d\boldsymbol{\omega}_i}{dt} = \sum_j \left(\boldsymbol{R}_i \times \boldsymbol{F}_{ij}^s - \mu_r R_i \left| \boldsymbol{F}_{ij}^n \right| \hat{\boldsymbol{\omega}}_i \right) \tag{2}$$

where $\boldsymbol{v}_i$, $\boldsymbol{\omega}_i$, and I_i are, respectively, the translational and angular velocities, and moment of inertial of particle i; $\boldsymbol{F}_{ij}^n$, $\boldsymbol{F}_{lj}^s$, and $\boldsymbol{F}_{ij}^l$ represent, respectively, the normal contact force, the tangential contact force, and the liquid-related force imposed on particle i by particle j. The first part of the right-hand side in Eq. 2 is the torque due to the tangential force, $\boldsymbol{F}_{ij}^s$, where $\boldsymbol{R}_i$ is a vector running from the center of the particle to the contact point with its magnitude equal to particle radius R_i. The second part is the resistant torque arising from rolling friction due to elastic hysteresis and losses or viscous dissipation, and μ_r is the coefficient of rolling friction (Tabor, 1955). This resistance has been shown to play a critical role in achieving physically or numerically stable results for unconfined packing, viz., the formation of a sandpile (Zhou et al., 1999) and implemented in our study of the packing of fine particles (Yang et al., 2000, 2002).

The contact mechanics between particles i and j can be calculated according to the Hertz theory for the normal force (Brilliantov et al., 1996) and Mindlin and Deresiewicz theory for the tangential force (1953). That is

$$\boldsymbol{F}_{ij}^n = \left[\frac{2}{3} E \sqrt{\overline{R}}\, \xi_n^{3/2} - \gamma_n E \sqrt{\overline{R}} \sqrt{\xi_n} \left(\boldsymbol{v}_{ij} \cdot \hat{\boldsymbol{n}}_{ij} \right) \right] \hat{\boldsymbol{n}}_{ij} \tag{3}$$

$$\boldsymbol{F}_{ij}^s = -\operatorname{sgn}(\xi_s)\, \mu_s \left| \boldsymbol{F}_{ij}^n \right| \left[1 - \left(1 - \min(\xi_s, \xi_{s,\max}) / \xi_{s,\max} \right) \right] \tag{4}$$

where parameter $E = Y/(1-\tilde{\sigma}^2)$; Y and $\tilde{\sigma}$ are the Young's modulus and the Poisson ratio; $\hat{\boldsymbol{n}}_{ij}$ is a unit vector running from the center of particle j to the center of particle i; $\overline{R} = R_i R_j/(R_i + R_j)$; γ_n is the normal damping coefficient; μ_s is the sliding friction coefficient; ξ_s is the total tangential displacement of particles during contact; and $\zeta_{s,\max} = \mu_s[(2-\bar{\sigma})/2(1-\tilde{\sigma})]\xi_n$ (Langston et al., 1995).

When a small amount of liquid is introduced, a pendular bridge can form between particles, as shown in Figure 1. The forces between particles due to the formation of a liquid bridge are both capillary and viscous in nature. The viscous force can become significant when the liquid viscosity is very high or at high interparticle velocities (Adams and Perchard, 1985). The present work considers the packing of glass beads wetted by water. As shown by Feng and Yu (1998) for such a packing system, the viscous force can be ignored. The capillary force, in the case where the gravitational distortion is negligible, contains two components: (1) the axial component of the surface tension acting on the three-phase contact line, and (2) the hydrostatic force evaluated from the reduced pressure in the liquid bridge, given by

$$\boldsymbol{F}_{ik}^l = -\left[2\pi\gamma R \sin\beta \sin(\beta + \phi) + \pi R^2 \Delta p \sin^2\beta \right] \hat{\boldsymbol{n}}_{ik} \tag{5}$$

Table 1. Parameters Used in the Simulation

Parameter	Value
Particle dia.	0.25, 1 mm
Particle density, ρ	2.5×10^3 kg·m^{-3}
Young's modulus, Y	1.0×10^7 N·m^{-2}
Poisson ratio, $\tilde{\sigma}$	0.29
Friction coeff., μ_s	0.3
Rolling friction coeff., μ_r	0.002
Normal damping coeff., γ_n	2×10^{-5} s^{-1}
Surface tension, γ	0.072 N·m^{-1}
Contact angle, ϕ	0

where γ is the liquid surface tension, β is the half-filling angle, and ϕ is the contact angle. The hydrostatic pressure within the bridge, Δp, is given by the Laplace–Young equation. However, analytical solutions to the Laplace–Young equation can be obtained only for very simple geometries. The toroidal approximation, proposed by Fisher (1926), treats the meniscus profile as a perfect circular arc, so Δp can be given by

$$\Delta p = \gamma\left(\frac{1}{r_1} - \frac{1}{r_2}\right) \tag{6}$$

where $r_1 = R[1 + s'](\sec\ \beta - 1]$, $r_2 = R[1 + (1 + s')\tan\ \beta - (1 + s')\sec\ \beta]$, and $s' = s/2R$. Equation 6 can estimate the capillary force with errors less than 10% for all stable separations and a wide range of bridge volumes (Lian et al., 1993). However, Eqs. 5 and 6 do not provide the liquid-bridge force as an explicit function of liquid-bridge volume and the separation distance, and are difficult to implement in DEM simulations. Simons et al. (1994) provided an equation for calculating liquid volume from the half filling angle, β, but their expression is quite lengthy and it is not convenient to calculate the half filling angle from the volume of a liquid bridge. Recognizing the problem, Weigert and Ripperger (1999) recently presented a much simpler explicit expression to relate liquid volume to the half filling angle, given by

$$V_l = 0.96R^3 \sin^4\beta(1 + 6s')(1 + 1.1\sin\phi) \tag{7}$$

The error of this expression is about 4% for a small amount of liquid, and the accuracy can be improved with a considerably more complex expression (Weigert and Ripperger, 1999). For simplicity, it is employed in the present work. To determine the liquid volume between two particles, however, we have to make an assumption of liquid distribution among particles in a packing. Two treatments were proposed in the previous work. Muguruma et al. (2000) assumed that the liquid can transport among particles and is distributed evenly among all gaps smaller than the rupture distance; on the other hand, Mikami et al. (1998) assumed the liquid is distributed evenly among particles and the liquid transport between particles can be neglected if the liquid viscosity is sufficiently small. By combining them together, in the present simulation, liquid is assumed to be distributed evenly to each particle and not transferable among particles; once the particle gap is smaller than the rupture distance, a liquid bridge is formed and the liquid assigned to a particle will be evenly distributed among its liquid bridges. According to Lian et al. (1993), the critical rupture distance s_{cri} is equal to $(1 + 0.5\phi)V_l^{1/3}$.

Simulation conditions

Glass beads and water are used in this work, following the experimental work of Feng and Yu (1998). A simulation begins with the random generation of monosize spherical particles with no overlap in a rectangular box. Each particle has a velocity of magnitude 0.01 m/s, but the direction is randomly assigned. To ensure consistent results, porosity at the initial state is constant, set to 0.8 for all packings. Then, as the packing process starts, the particles begin to settle down under gravity and during this densification process, they collide with neighboring particles and bounce upward or downward. This dynamic process proceeds until all particles reach their stable positions with an essentially zero velocity as a result of the damping effect for energy dissipation. This packing process is approximately equivalent to a physical operation to transform a fluidized bed to a fixed bed by stopping gas supply. Periodical boundary conditions are applied along two horizontal directions to avoid lateral wall effect.

Table 1 lists the parameters used in the simulation. Note that Young's modulus in the present study is four orders of magnitude smaller than the typical value of 10^{11} N·m^{-2} for glass beads to reduce computational effort. This treatment has also been used in our previous work and found to have a negligible effect on the final results. Our previous study also showed that the packing of particles of sizes less than 0.1 mm is strongly affected by the van der Waals force (Yang et al., 2000). Therefore, as our first step to understand the effect of capillary force on packing structure, the minimum size of particle used in this work is 0.25 mm, to avoid the possible effect of the van der Waals force.

Different liquid additions are used in the simulation in order to understand the effect of capillary force. Three main states are usually observed in the randomly packed particles according to the amount of liquids, namely, the pendular, funicular, and capillary states (Newitt and Conway-Jones, 1958). The pendular state corresponds to low moisture content in a packing where liquid is held as discrete lenticular rings at the contacts between particles. At high moisture content, the rings may coalesce, forming a continuous network of liquid, giving the so-called funicular state. A further increase in moisture content leads to the capillary state, in which the pores among particles are completely filled with liquid. According to Flemmer (1991), for monosized spheres, these states correspond

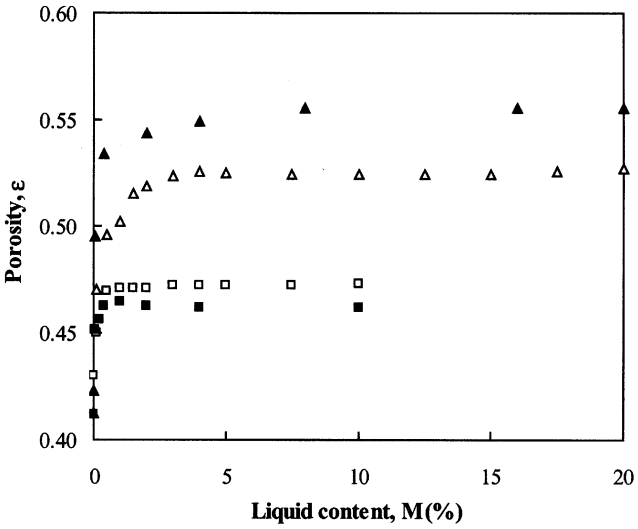

Figure 2. Porosity as a function of liquid content (water) for the packing of 1-mm (■) and 0.25-mm (▲) particles.

The experimental results of 1-mm (□) and 0.25-mm (△) particles are also plotted for comparison.

to a certain liquid content M, here defined as the weight percentage of water to glass beads

Pendular regime

$$0 < M\ (\%) < 9.2$$

Funicular regime

$$9.2 < M\ (\%) < 26.7$$

Capillary regime

$$M\ (\%) \geq 26.7$$

These values were obtained from the geometrical analysis of the liquid state in a static packed bed, with porosity assumed to be 0.4. However, forming a packing is actually a dynamic process that may produce a porosity much larger than 0.4. In this case, the pendular and funicular regimes may be larger, as noted by Feng and Yu (1998). In the present study, the liquid content, M, varies from zero to 20%. Therefore, the present study mainly covers the pendular regime, with a small extension to the funicular regime where the capillary force is still very important.

Results and Discussion

Validity of the DEM model

Figure 2 shows the dependence of porosity, ϵ, on liquid content, M. To be consistent with the previous work (Feng and Yu, 1998, 2000; Zou et al., 2001), the porosity is the so-called dry-based porosity, defined as the ratio of the total volume of voids and liquid to the volume of the whole packing. It can be seen that the $\epsilon - M$ relationship for the packings of either 0.25- or 1-mm particles shows a similar pattern: porosity increases rapidly with liquid content to a critical point, after which porosity is insensitive to M. The maximum porosity is 0.550 at $M = 2.5\%$ for 0.25-mm particles and 0.465 at $M = 0.8\%$ for 1-mm particles, showing that the packing of smaller-sized particles produces a more profound increase in porosity and a wider increasing region. As a matter of fact, if the particle size is large enough, the effect of liquid may not be observed, yielding a porosity that is the same as that of dry particles (Feng and Yu, 1998). For the purpose of comparison, the measured data from Feng and Yu (1998) were also plotted in Figure 2, showing that the present simulation can largely reproduce the measured $\epsilon - M$ relationship. It is noted, however, that the simulated results quantitatively differ from the measured data. There are a few factors responsible for this difference. First, the packing method used in the simulation is not exactly the same as that in the experiment. Second, in the simulation, the liquid is assumed to distribute evenly among particles. In reality, the situation is much more complicated and the distribution is certainly not uniform. Third, the equations used to calculate the interparticle forces, including the one for capillary force, are all obtained under ideal conditions, which may not fully represent the reality.

Feng and Yu (1998) proposed a two-region model that to some degree corresponds to the pendular and funicular states

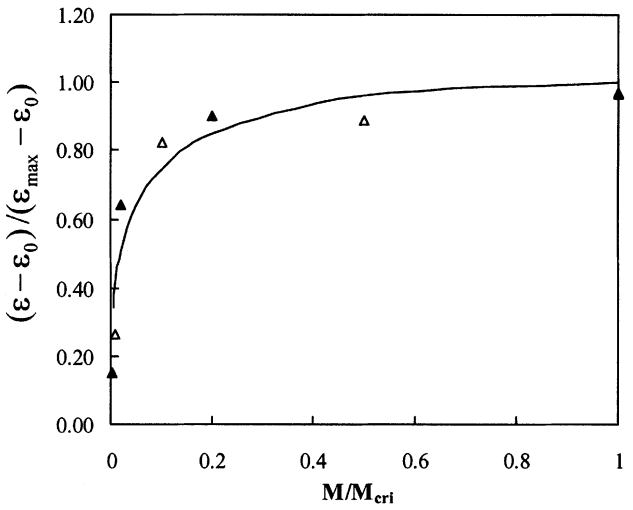

Figure 3. Normalized relationship between porosity and liquid content for the packing of 0.25-mm (▲) and 1-mm (△) particles; the line is calculated by Eq. 8.

to describe the $\epsilon - M$ relationship: a wetting region where porosity increases with liquid addition and a filling region in which the porosity is independent of liquid addition and remains constant. There is another region called the slurry/sediment region where porosity decreases with liquid content because excess liquid will gradually eliminate the capillary force. Focusing on the first two regions, they found that the $\epsilon - M$ relationship can be characterized by three parameters: initial porosity ϵ_0 corresponding to the packing of dry particles, maximum achievable porosity ϵ_{max}, and its corresponding liquid content, M_{cri}. When all the porosity results were expressed as $(\epsilon - \epsilon_0)/(\epsilon_{max} - \epsilon_0)$ and then plotted against M/M_{cri}, there is a general relationship between the two variables, which can be described by the following equation (Feng and Yu, 1998)

$$\frac{\epsilon - \epsilon_0}{\epsilon_{max} - \epsilon_0} = \left(\frac{M}{M_{cri}}\right)^{0.423}\left[1 - 0.421\ \ln\left(\frac{M}{M_{cri}}\right)\right] \qquad (8)$$

where ϵ_0 is constant for a given method, 0.4 for loose random packing, and ϵ_{max} and M_{cri} are dependent on the particle and liquid properties. This normalized equation, facilitated by other equations to calculate ϵ_{max} and M_{cri}, can provide an effective way for predicting the $\epsilon - M$ relationship for different types of liquid and/or particles. To further confirm the validity of the proposed model, we plotted our simulated data in Figure 3 in this way. The parameters of ϵ_0, ϵ_{max}, and M_{cri} obtained from the simulation are, respectively, 0.393, 0.549, and 2.5% for the packing of 0.25-mm particles, and 0.393, 0.4645, and 0.8% for the packing of 1-mm particles. It is observed that our simulated data agree quite well with Eq. 8. The agreement between simulated and measured results macroscopically verifies the present simulation technique, at least qualitatively, providing a good basis for the

analysis of packing and force structures, which are difficult to obtain experimentally.

Characterization of the packing structure

One of the advantages of the DEM simulation is that it is quite straightforward to provide the microscopic, structural information of a packing, such as the radial distribution function, $g(r)$, and coordination number, C_n. Figure 4 shows the $g(r)$, functions for 1- and 0.25-mm particles with different liquid contents. For the packing of dry coarse particles, as shown in our previous study (Yang et al., 2000), the $g(r)$ curves of both-sized particles show all the well-known short-range features observed in the random packing of particles (Finney, 1970). The features can also be found in the packing with a small amount of liquid ($M = 0.004\%$ in Figures 4a and 4b). In particular, their second peaks have a subpeak at $r = 1.73$, corresponding to edge-sharing in-plane equilateral-triangle structure. This type of particle connection is recognized as a key characteristic of a random close packing of hard spheres (Finney, 1970). With the addition of more liquid, the $g(r)$ curve of 1-mm particles has little change except for a slight increase in the first peak (Figure 4a). On the other hand, the addition of liquid has more impact on the $g(r)$ function of 0.25-mm particles. As shown in Figure 4b, as the liquid content increases, its first peak becomes narrower, with a sharp decrease in the first minimum; the subpeak at $r = 1.73$ and peaks beyond the second peak also gradually vanish. In the packing of fine particles where the van der Waals force is significant, Yang et al. (2000) observed a similar change when porosity increases as a result of decreasing particle size. The results in Figure 2 indicate that porosity increases when the liquid content increases. Therefore, the variation of $g(r)$ is largely consistent with the change in porosity, insensitive to the method of generating such a change.

The coordination number, that is, the number of "contacts" made by a particle, is a more sensitive measure of the local structure. It varies significantly with the critical distance of separation, less than which two particles are defined to be in contact. Figure 5 shows the frequency distribution of coordination number, C_n, when the critical distance of separation is set to a particle diameter of 1.005, a value that has been used in our study of the packing of fine particles (Yang et al., 2000). For 1-mm particles, the C_n of all packings with different liquid contents varies from 3 to 9, and its frequency distribution is approximately symmetrical with its most probable value at 6, which is obviously comparable with the previous results (Finney, 1970; Liu et al., 1999; Yang et al., 2000). This is consistent with the porosity and $g(r)$ results discussed earlier. For the packing of 0.25-mm particles, the C_n distribution clearly shifts to the lower side with liquid addition, giving an obviously decreased mean value. However, a further increase in liquid content (that is, $M = 20\%$) shifts the distribution back to give a higher mean value.

Figure 6 shows the variation of the mean coordination number, $< C_n >$, with liquid content for 0.25-mm particles.

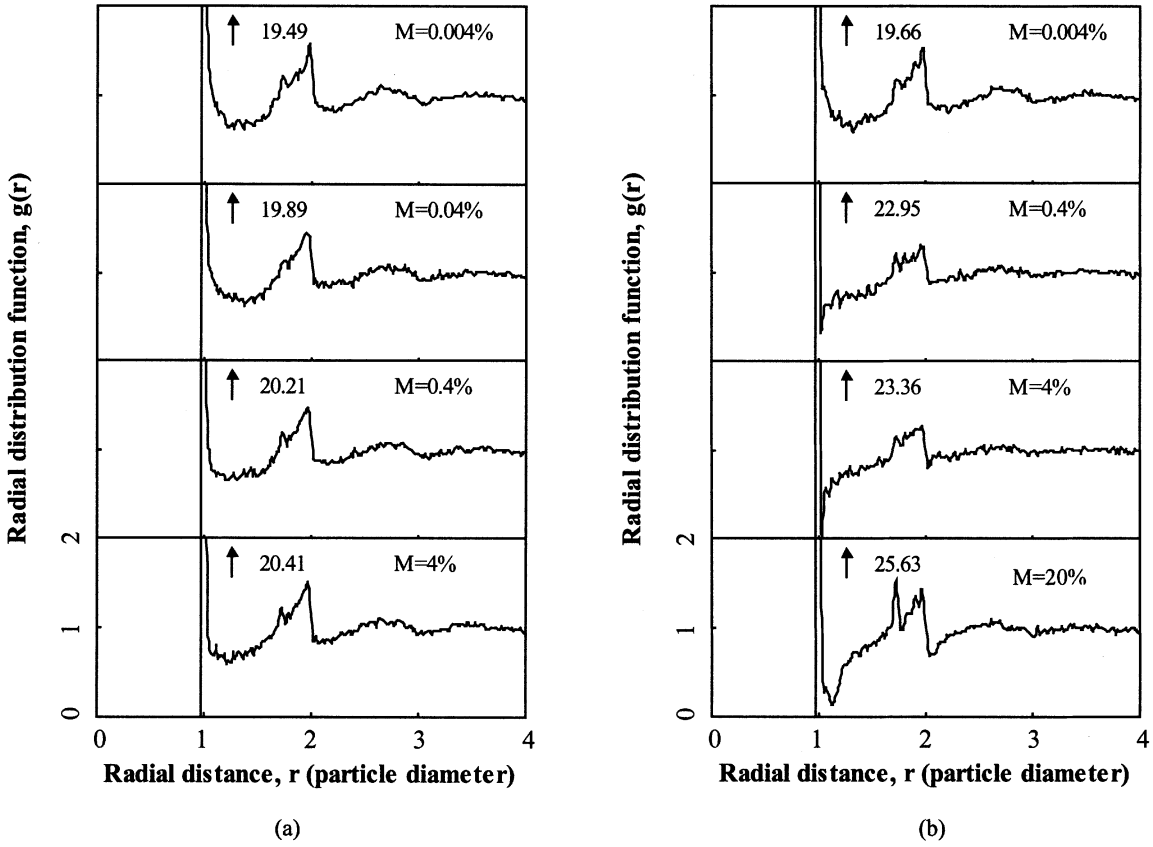

Figure 4. Radial distribution function at different liquid contents for (a) 1-mm, and (b) 0.25-mm particles.

It is a common knowledge from the previous work that for monosized spheres, the mean coordination number decreases with increasing porosity (German, 1989; Pinson et al., 1998; Yang et al., 2000). However, this trend is not observed for wet particles if one examines the results in Figure 6 with those in Figure 2.

Figure 7 shows the internal packing structures of 0.25-mm particles. It is observed that the packing of dry particles ($M = 0.0\%$) has a quite homogenous structure. With the addition of liquid up to about $M = 2.5\%$, arches are formed in parallel with the increased capillary force; the packing structure is still uniform, but looser compared to that at $M = 0.0\%$. With a further increase of liquid content, some particles pack closely to form locally stable agglomerates. When agglomerates are formed, the packing structure is less homogeneous and two kinds of structure, namely intra-agglomerate and interagglomerate can be identified (German, 1989; Yu et al., 1995). The particles in an agglomerate are relatively closely packed and, hence, have high $< C_n >$, but the development of an interagglomerate structure gives a high porosity. The formation of agglomerates is responsible for the observed increase in $< C_n >$ at high liquid content at individual contact and/or particle scale.

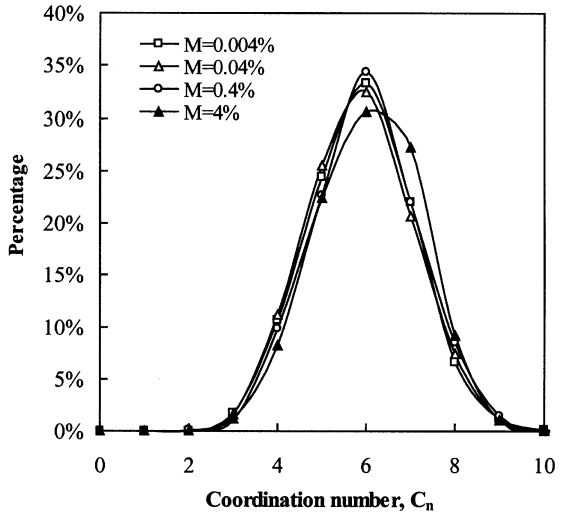

(a)

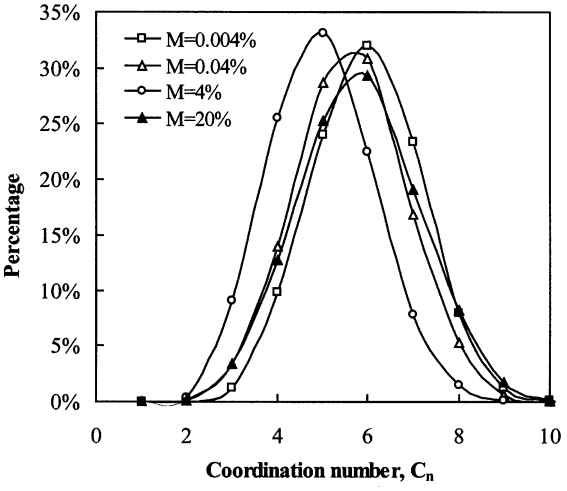

(b)

Figure 5. Coordination number distribution at different liquid contents for (a) 1-mm, and (b) 0.25-mm particles.

Characterization of the force structure

For the packing of wet particles, it is useful to quantify the relationship between bulk properties, for example, porosity, and interparticle forces. In general, two approaches can be used for this propose: the macroscopic approach, which is based on well-established theories and understanding and supported by experimental measurement (Feng and Yu, 1998), and the microscopic approach, which is mainly achieved by dynamic simulation (Yang et al., 2000). In the present DEM simulation, the contact and capillary forces can be explicitly obtained, so it is possible to study how they vary with liquid content at a microscopic level.

Figure 8 shows the spatial distribution or network of the normal contact forces, $\boldsymbol{F}^n$, within the packings at different liquid content, where the centers of two contact particles are linked by sticks of different thickness, which is proportional to the magnitude of $\boldsymbol{F}^n$. Note that for better illustration at a given liquid content, M, the scale used in Figure 8 is not the same for different liquid contents. For the packing of dry particles (that is, $M = 0.0\%$), the distribution is heterogeneous with the force chains propagating upward because of the effect of gravity, giving a so-called force-arching phenomenon as experimentally observed in 2-D packing (Liu et al., 1995; Mueth et al., 1998). At $M = 0.04\%$, the force arching is less obvious, implying that the role of the gravity force relative to the capillary force decreases. As the liquid content increases to $M = 4\%$, the liquid force gradually becomes comparable with the gravity force; consequently, the network distribution of the contact forces is more uniform, both in space and magnitude. With a further increase in liquid content to $M = 20\%$, the localized strong capillary forces are significant; corresponding to this is the existence of the strong contact forces and formation of agglomerates, and the strong force chains are often found within and through the agglom-

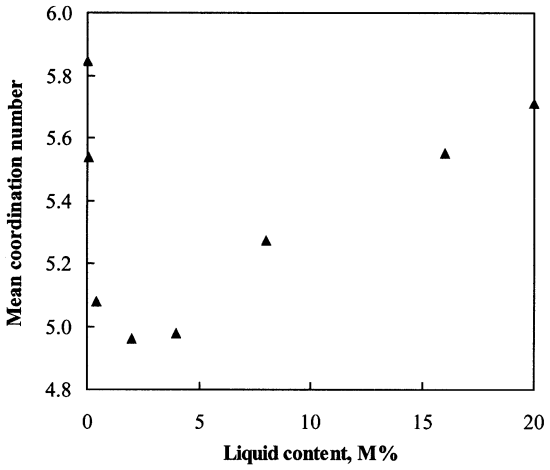

Figure 6. Mean coordination number $< C_n >$ as a function of liquid content for 0.25-mm particles.

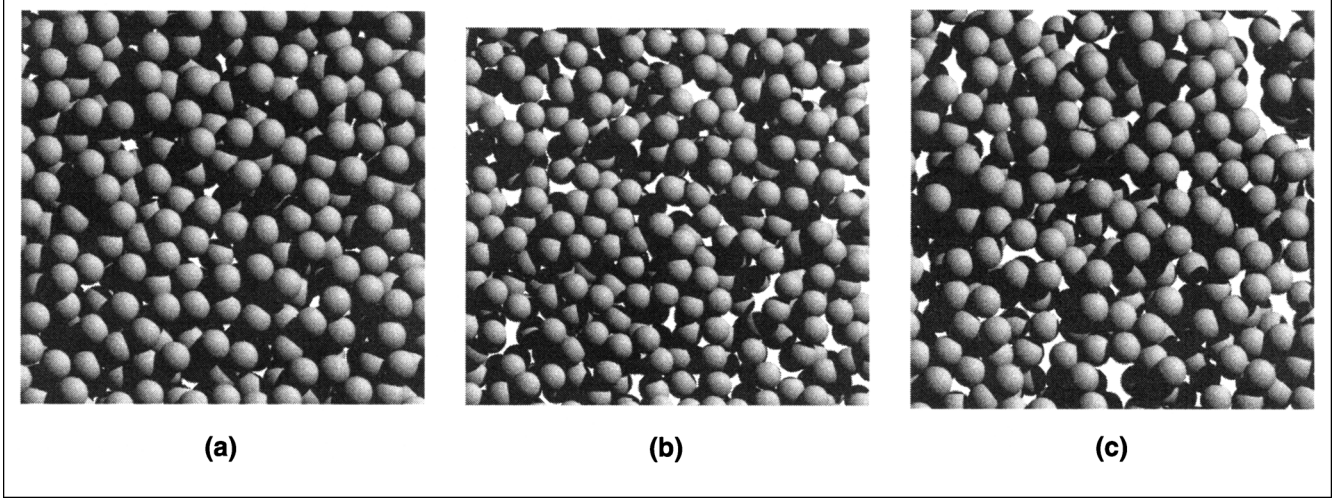

Figure 7. Internal packing structure of a thin layer of 1.9 particle diameter thickness for 0.25-mm particles at different liquid contents: (a) $M = 0.0\%$, (b) $M = 2\%$, and (c) $M = 20\%$.

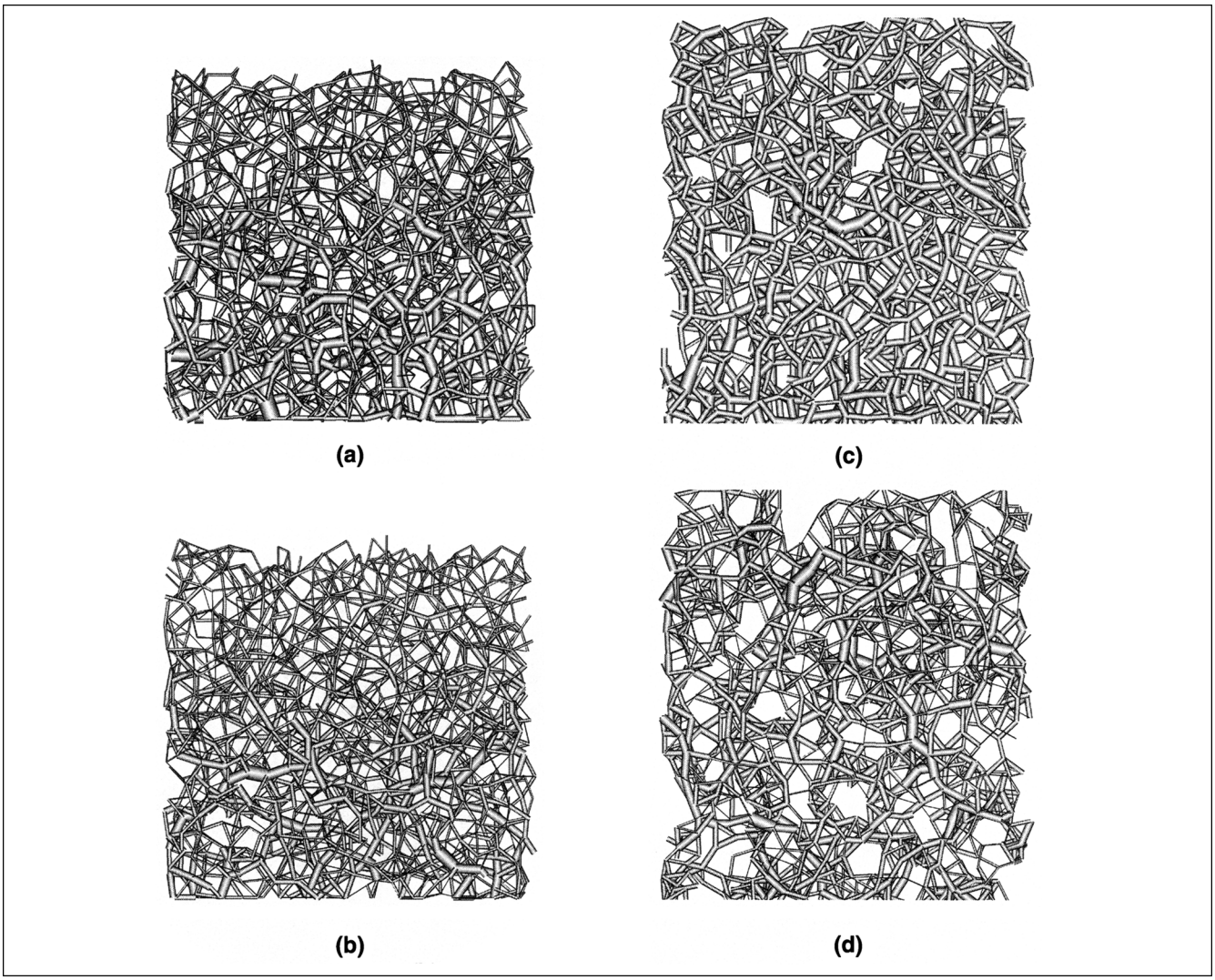

Figure 8. Network of the normal contact forces of a thin layer of 1.9 particle diameter thickness for 0.25-mm particles at different liquid contents: (a) $M = 0.0\%$, (b) $M = 0.04\%$, (c) $M = 4\%$, and (d) $M = 20\%$.

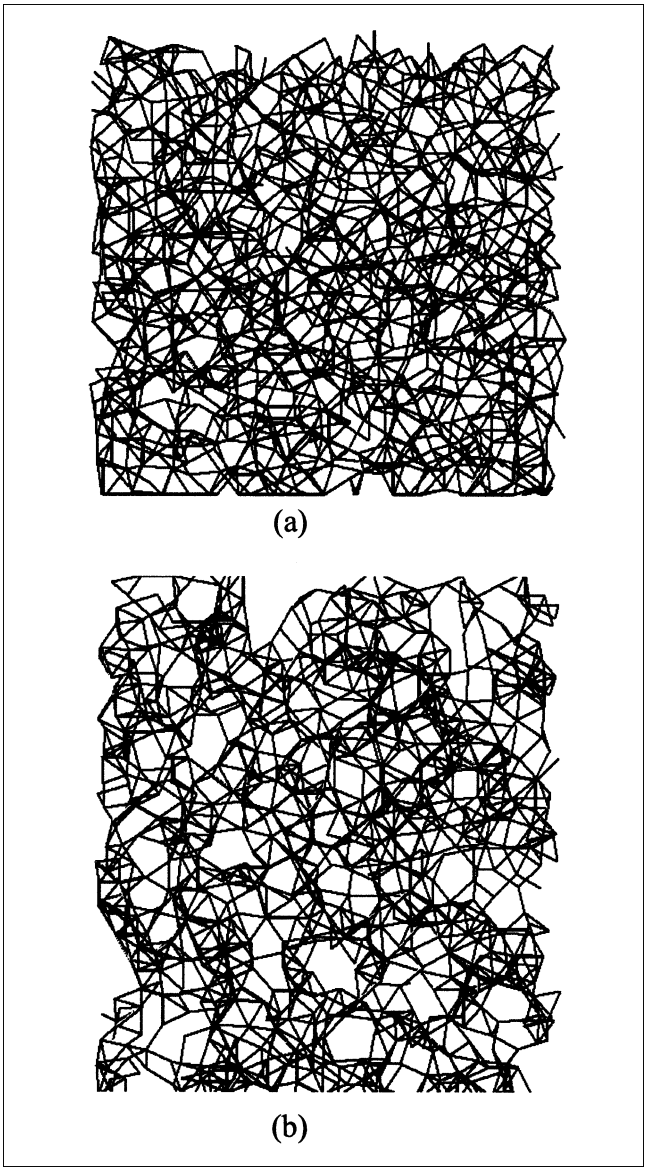

Figure 9. Network of the capillary forces of a thin layer of 1.9 particle diameter thickness for 0.25-mm particles at different liquid contents: (a) M = 0.04%, and (b) M = 20%.

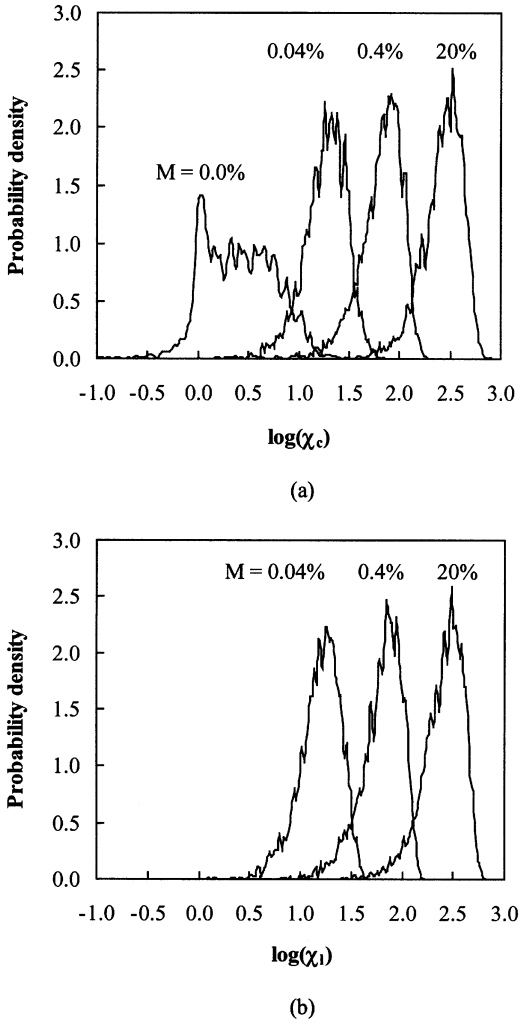

Figure 10. Probability density distribution of: (a) contact forces; and (b) capillary forces relative to the gravity force for the packing 0.25-mm particles as a function of liquid content.

erates. The force structure is directly linked to the packing structure. In fact, the nonuniform packing structure at M = 20% shown in Figure 8d is probably more illustrative than in Figure 7c.

The capillary force provides an extra cohesive force in stabilizing a packing by restricting the relative movement of particles. It exists if the distance between two particles is less than the rupture distance, so that its force network is very much the same as that of the contact force, as shown in Figure 9. However, it is found that compared to the contact force, the magnitude of the capillary force does not vary much, giving a rather uniform distribution in magnitude.

Similar to our previous study of the packing of fine particles, two force ratios are used in this work for quantitative analysis, defined by

$$\chi_l = \left| \sum_j \boldsymbol{F}_{ij}^l \right| / m_i g \tag{9}$$

and

$$\chi_l' = \sum_j \left| \boldsymbol{F}_{ij}^l \right| / m_i g \tag{10}$$

The two definitions are also applied to the contact force $\boldsymbol{F}_{ij}^c$. Figure 10 shows the probability density distributions of the contact and capillary forces for the packing of 0.25-mm particles at different liquid contents. They are in terms of Eq. 9, but with logarithmic scale. Similar distributions are found in terms of Eq. 10. As expected, the capillary force relative to the gravity force in a packing increases with the increase in liquid content. The ratio of the contact force to the gravity

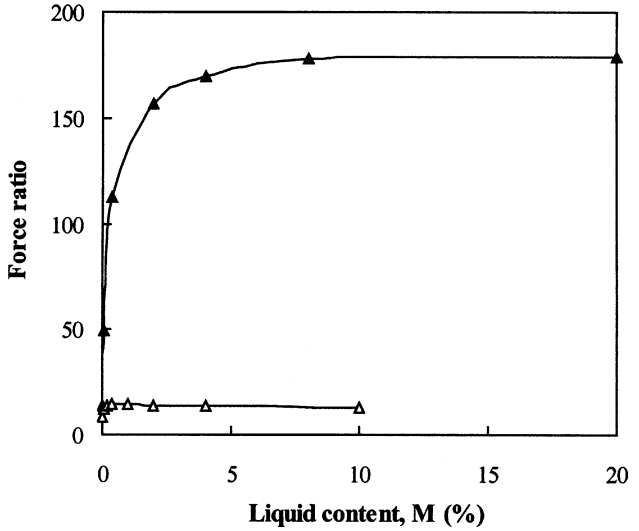

Figure 11. Dependence of the force ratio χ_l' on the liquid content for the packing of 0.25-mm (▲) and 1-mm (△) particles.

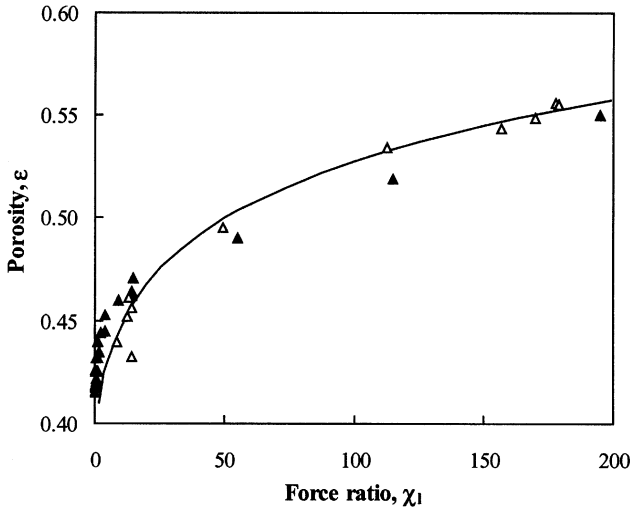

Figure 12. Porosity as a function of the force ratio χ_l, obtained from the simulation (△) and experiment (▲).

The line is the result from Eq. 9, with parameters $\epsilon_0 = 0.393$, $m = -3.88$ and $n = -0.21$.

force will accordingly increase in order to create a repulsive force to maintain the mechanical equilibrium. Another important feature here is that the contact force distributions become more similar to the capillary force distribution as liquid content increases. This similarity reflects the dominant role of the capillary force, as the contact force is the passive force and can only respond to the active force, that is, the capillary force in this case.

In Figure 11 the mean value of χ_l' is plotted against liquid content, which shows that the capillary force increases with the addition of water to a maximum value after which the force is independent of liquid addition. It is also found that the increasing region of the capillary force is much larger for 0.25-mm particles. The variation in capillary force with liquid content is quite similar to that of porosity with liquid content, as shown in Figure 2. The liquid content giving the maximum force ratio, χ_l', in Figure 12 corresponds to M_{cri}, and a high force ratio for the packing of the 0.25-mm particles results in a high porosity. The results confirm, from the microscopic point view, the argument proposed by Feng and Yu (1998) that porosity should be related to the capillary force for wet particles.

It was reported that the relationship between porosity and interparticle forces can be described by the following equation (Feng and Yu, 2000; Yang et al., 2000)

$$\epsilon = \epsilon_0 + (1 - \epsilon_0)\exp(m\chi_l^n) \tag{11}$$

where ϵ_0 is the porosity when the interparticle forces can be completely negligible. Figure 12 presents the porosity, ϵ, as a function of the force ratio, χ_l. Data from the present simulation and those from Feng and Yu (2000) have been plotted together for comparison. It clearly shows that our simulated data agree quite well with those from the previous work (Feng and Yu, 2000), indicating that the macroscopic and microscopic approaches are consistent with each other although each approach involves assumptions or treatments that are not fully verified at present. This is also consistent with the previous analysis of the packing of fine particles (Yang et al., 2000). Therefore, there may be a general relationship between porosity and interparticle force for commonly used particles, as proposed by Yu et al. (2003). However, it should be pointed out that if there is a very significant change in surface properties of materials, the $\epsilon - \chi_l$ relationship may vary (Yang et al., 2003). So further study is necessary in order to develop a comprehensive understanding of the role of interparticle forces and the $\epsilon - \chi_l$ relationship.

Conclusions

A DEM-based numerical model has been developed to study the packing of wet particles. In the proposed model the capillary force, like the contact forces, is explicitly considered. Simulations have been performed for glass beads of diameters 0.25 and 1 mm with different moisture contents. The results indicate the following.

- Porosity increases with liquid addition in the wet region, but remains constant in the filling region. The packing of smaller-sized particles has a wider wetting region. The normalized equation, that is, Eq. 8, can describe the $\epsilon - M$ relationship well. The simulated results are in reasonably good agreement with the measured data under comparable conditions, confirming the validity of the proposed model in the study of packing of wet particles.
- The radial distribution function varies with liquid content, in line with porosity. For the packing of dry particles, it has a clear split-second peak, like that observed in the previous work. However, as liquid content increases, the first peak becomes narrower and higher, and the first subpeak of the split-second peak gradually vanishes.
- The mean coordination number decreases to a minimum value and then increases with liquid content for small parti-

cles. Agglomerates can form in a packing at high liquid content. This produces a less homogeneous packing structure, and the packing properties will depend on intra-agglomerate and interagglomerate structures. The formation of agglomerates results in an increase in the mean coordination number at high liquid content.

- Force chains, representing the contact forces among particles, are observed in the packing of dry or wet particles. The force structure becomes more uniform as liquid content increases, because of the increasing capillary force. However, a further increase in liquid content will result in heterogeneous force structures where the strong force chains are often found within and through the agglomerates. The force network of capillary forces among particles corresponds to that of contact forces, although the magnitude of the capillary force does not vary as much.

- The relationship between porosity and the capillary force relative to particle weight in the present work is consistent with the previous experimental work and can be described by the simple equation give by Eq. 11.

Acknowledgment

The authors are grateful to the Australia Research Council and the University of New South Wales for financial support of this work.

Notation

Δp = hydrostatic pressure, $N \cdot m^{-2}$
$\boldsymbol{F}^l$ = liquid force, N
$\boldsymbol{F}^n$ = normal contact force, N
$\boldsymbol{F}^s$ = sliding contact force, N
I = moment of inertial, $kg \cdot m^2$
M = mass ratio of liquid to particle
m = particle mass, kg
R = particle radius, m
s = surface gap between particles, m
υ = translational velocity, $m \cdot s^{-1}$
Y = Young's modulus, $N \cdot m^{-2}$

Greek letters

β = half-filling angle, deg
χ_c = ratio of contact force to particle weight, defined by Eq. 9
χ_l = ratio of capillary force to particle weight, defined by Eq. 9
χ_l' = ratio of capillary force to particle weight, defined by Eq. 10
ϵ = porosity
ϕ = contact angle, degree
γ = liquid surface tension, $N \cdot m^{-1}$
γ_n = normal damping coefficient
μ_r = rolling friction coefficient
μ_s = sliding friction coefficient
ρ = particle mass density, $kg \cdot m^{-3}$
$\tilde{\sigma}$ = Poisson ratio
ω = angular velocity, s^{-1}
ξ_n = normal displacement, m
ξ_s = total tangential displacement, m
$\xi_{s,\max}$ = maximum tangenital displacement, m

Literature Cited

Adams, M. J., and V. Perchard, "The Cohesive Forces Between Particles with Interstitial Liquid," *Int. Chem. Eng. Symp. Ser.,* **91**, 147 (1985).

Bideau, D., and A. Hansen, *Disorder and Granular Media,* Elsevier, North-Holland, Amsterdam, The Netherlands (1993).

Brilliantov, N. V., F. Spahn, J. M. Hertzsch, and T. Pöschel, "Model for Collisions in Granular Gases," *Phys. Rev. E,* **53**, 5382 (1996).

Cundall, P. A., and O. D. L. Stack, "A Discrete Numerical Model for Granular Assemblies," *Geotechnique*, **29**, 47 (1979).

Feng, C. L., and A. B. Yu, "Effect of Liquid Addition on the Packing of Mono-Sized Coarse Spheres," *Powder Technol.,* **99**, 22 (1998).

Feng, C. L., and A. B. Yu, "Quantification of the Relationship Between Porosity and Interparticle Forces for the Packing of Wet Uniform Spheres," *J. Colloid Interface Sci.,* **231,** 136 (2000).

Finney, J. L., "Random Packings and the Structure of Simple Liquids: I. The Geometry of Random Close Packing," *Proc. Roy. Soc. London A,* **319,** 479 (1970).

Fisher, R. A., "On the Capillary Forces in an Ideal Soil, Correction of Formulate Given by W.B. Haines," *J. Agric. Sci.*, **16**, 492 (1926).

Flemmer, C. L., "On the Regime Boundaries of Moisture in Granular Materials," *Powder Technol.*, **66**, 191 (1991).

German, R. M., *Particle Packing Characteristics,* Metal Powder Industries Federation, Princeton, NJ (1989).

Hinkley, J., A. G. Waters, D. O'Dea, and J. D. Lister, "Voidage of Ferrous Sinter Beds: New Measurement Technique and Dependence on Feed Characteristics," *Int. J. Miner. Process.*, **41**, 53 (1994).

Krupp, H., "Particle Adhesion Theory and Experiment," *Adv. Colloid Interface Sci.,* **1**, 111 (1967).

Langston, P. A., U. Tüzün, and D. M. Heyes, "Discrete Element Simulation of Granular Flow in 2D and 3D Hoppers: Dependence of Discharge Rate and Wall Stress on Particle Interactions," *Chem. Eng. Sci.,* **50**, 967 (1995).

Lian, G., C. Thornton, and M. J. Adams, "A Theoretical Study of the Liquid Bridge Forces Between Two Rigid Spherical Bodies," *J. Colloid Interface Sci.,* **161**, 138 (1993).

Liu, C.-H., S. R. Nagel, D. A. Schecter, S. N. Coppersmith, S. Majumdar, S. Narayan, and T. A. Witten, "Force Fluctuations in Bead Packs," *Science,* **269,** 513 (1995).

Liu, L. F., Z. P. Zhang, and A. B. Yu, "Dynamic Simulation of the Centripetal Packing of Particles," *Physica A,* **268,** 433 (1999).

Metha, A., *Granular Matter: An Interdisciplinary Approach,* Springer-Verlag, New York (1994).

Mikami, T., H. Kamiya, and M. Horio, "Numerical Simulation of Cohesive Powder Behaviour in a Fluidized Bed," *Chem. Eng. Sci.,* **53**, 1927 (1998).

Mindlin, R. D., and H. Deresiewicz, "Elastic Spheres in Contact Under Varying Oblique Forces," *J. Appl. Mech.,* **20**, 327 (1953).

Mueth, D. M., H. M. Jaeger, and S. R. Nagel, "Force Distribution in a Granular Medium," *Phys. Rev. E,* **57**, 3164 (1998).

Muguruma, Y., T. Tanaka, S. Kawatake, and Y. Tsuji, "Numerical Simulation of Particulate Flow with Liquid Bridge Between Particles (simulation of a centrifugal tumbling granulator)," *Powder Technol.,* **109,** 49 (2000).

Newitt, D. M., and J. M. Conway-Jones, "A Contribution to the Theory and Practice of Granulation," *Trans. Inst. Chem. Eng.,* **36**, 422 (1958).

Pinson, D., R. P. Zou, A. B. Yu, P. Zulli, and M. McCarthy, "Coordination Number of Binary Mixtures of Particles," *J. Phys. D: Appl. Phys.,* **31**, 457 (1998).

Rumpf, H., "The Strength of Granules and Agglomerates," *Agglomeration,* W. A. Knepper, ed., Wiley-Interscience, New York (1962).

Simons, S. J. R., J. P. K. Seville, and M. J. Adams, "An Analysis of the Rupture Energy of Pendular Liquid Bridges," *Chem. Eng. Sci.,* **49**, 2331 (1994).

Tabor, D., "Mechanism of the Rolling Friction," *Proc. Roy. Soc. A,* **229,** 198 (1955).

Visser, J., "Van der Waals and Other Cohesive Forces Affecting Powder Fluidization," *Powder Technol.,* **58**, 1 (1989).

Weigert, T., and S. Ripperger, "Calculation of the Liquid Bridge Volume and Bulk Saturation from the Half-Filling Angle," *Part. Part. Syst. Charact.,* **16**, 238 (1999).

Yang, R. Y., R. P. Zou, and A. B. Yu, "Computer Simulation of Packing of Fine Particles," *Phys. Rev. E,* **62**, 3900 (2000).

Yang, R. Y., R. P. Zou, and A. B. Yu, "Effect of Material Properties on the Packing of Fine Particles," *Powder Technol.* in press (2003).

Yang, R. Y., R. P. Zou, and A. B. Yu, "Voronoi Tessellation of the Packing of Fine Uniform Spheres," *Phys. Rev. E,* **65** (2002).

Yu, A. B., J. Bridgwater, and A. Burbidge, "On the Modelling of the Packing of Fine Particles," *Powder Technol.,* **92**, 185 (1997).
Yu, A. B., C. L. Feng, R. P. Zou, and R. Y. Yang, "On the Relationship Between Porosity and Interparticle Forces," *Powder Technol.,* 130, 70 (2003).
Yu, A. B., N. Standish, and L. Lu, "Coal Agglomeration and Its Effect on Bulk Density," *Powder Technol.,* **82**, 177 (1995).
Yu, A. B., and R. P. Zou, "Prediction of the Porosity of Particle Mixtures: A Review," *KONA Powder Part.,* **16**, 68 (1998).
Zhang, Z. P., L. F. Liu, Y. D. Yan, and A. B. Yu, "A Simulation Study of the Effects of Dynamic Variables on the Packing of Spheres," *Powder Technol.,* **116,** 23 (2001).
Zhou, Y. C., B. D. Wright, R. Y. Yang, B. H. Xu, and A. B. Yu, "Rolling Friction in the Dynamic Simulation of Sandpile Formation," *Physica A,* **269,** 536 (1999).
Zou, R. P., C. L. Feng, and A. B. Yu, "The Packing of Binary Mixture of Wet Coarse Spheres," *J. Amer. Ceram. Soc.,* **84**, 504 (2001).

Manuscript received June 28, 2002, revision received Dec. 16, 2002, and final revision received Feb. 18, 2003.